DYNAMIC SIMULATION OF A TOWED DECOY SYSTEM

Martin Carlsson Leijonhufvud and Anders Lindberg
Saab AB, SE-581 88, Linkoping, Sweden

Abstract

A recently developed simulation tool for towed decoy systems is presented and evaluated. First, the numerical modeling approach for the wire dynamics is outlined and the results from some basic simulations are described. The numerical model is then implemented into a simulator and an example of application considering the design of a towed decoy system is presented. Focus is not only on the dynamics of the wire and decoy as a separate system but also on the interaction with the aircraft and the disturbed flow behind the aircraft where the slipstream from the engine and propellers play an important role .

1   Introduction

There are a wide range of aeronautical applications where wires and cables are used for towing purposes [1]. Examples of such applications are towed decoys and sensors, air target towing, air-to-air refueling, water bombing, and precision target delivery.

When it comes to design and analysis of a towed wire system, a numerical simulation capability of the wire dynamics is often a necessity in order to reduce development time and cost. There are several suggested approaches for modeling of wire dynamics [1], [2], [3], [4]. In general, the methods can be divided into two main categories referred to as continuum models and lumped mass models [5]. The continuum approach is sometimes claimed to be the more accurate, whereas the lumped mass method usually offers significant advantages in terms of simplicity and implementation [6].

In this paper, a three-dimensional (3D) lumped-mass elastic wire model is developed and described. This type of numerical representation is found to be a good choice with respect to the simulation objectives and the programming considerations in mind. The aerodynamics of the wire is modeled using a quasi-steady approach based on the cross flow principle [7]. The equations of motion for the wire system are described in the paper and the state-space equations suitable for implementation are given. Results from some basic simulations are also given for comparison and evaluation purposes.

The wire model is also implemented into a special simulation tool developed by Saab that is mainly used for stores separation analysis. An example considering analysis of a towed decoy system is presented and discussed. The dynamics of the wire is here coupled to the motion of the aircraft and the dynamics of the decoy itself. Furthermore, the disturbed flow behind the aircraft is modeled based on wind tunnel data. This detail is found to be crucial in order to perform representative simulations.

2   Numerical Modeling

The purpose of the numerical model is to enable simulation of arbitrary wire motion in the 3D space. The equations of motion for the wire system are in the following formulated using an earth-fixed coordinate system.

Structural Dynamics

The structure of the wire is discretely represented by a series of connected elastic wire (or spring) elements according to Fig. 1.

The mass of the wire is approximated using point masses (m_i) located at the nodes (points of connection) between the wire elements. The degrees of freedom, $\mathbf{w}$, for the wire system are hence the 3D positions of the mass elements in the earth fixed coordinate system.
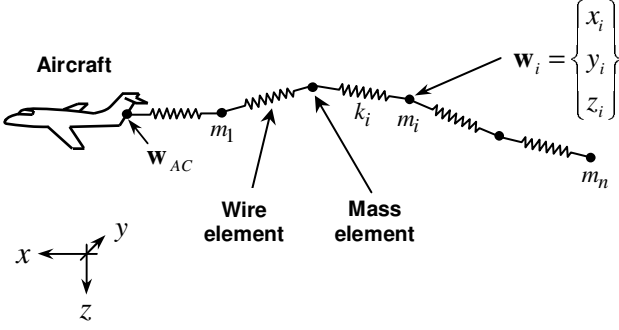
Fig. 1: Illustration of wire model.

The equations of motion for the i:th mass element may be expressed as

$$m_i \ddot{\mathbf{w}}_i - \mathbf{f}_{e,i}(\mathbf{w}) - m_i \mathbf{g}_i - \mathbf{f}_{a,i}(\mathbf{w}, \dot{\mathbf{w}}) = \mathbf{0}, \qquad (1)$$

where a dot denotes differentiation with respect to time t. The first term represent the acceleration forces and the second term is the vector of elastic forces acting on the mass element. The third term is the gravity forces and the last term represents the vector of aerodynamic forces. Structural damping forces (internal wire friction) are, for the current application, excluded since these forces are estimated to be very small compared to the other involved forces. It is however straightforward to include damping forces by applying viscoelastic elements as described in Ref. [1].

The acceleration forces are simply the mass of the i:th mass element times the three-dimensional vector of mass element acceleration. The vector of elastic forces can be found by studying Fig. 2. The vector $\mathbf{v}_i$ here denotes the vector pointing from point $\mathbf{w}_i$ to the previous point $\mathbf{w}_{i-1}$ (towards the aircraft). Hence, the following holds:

$$\mathbf{v}_i = \mathbf{w}_{i-1} - \mathbf{w}_i, \qquad i = 2:n, \qquad (2A)$$

where n is the total number of elements. A special condition holds for the first mass element where the position $\mathbf{w}_{i-1}$ correspond to the position of the point of wire attachment to the aircraft called $\mathbf{w}_{AC}$ (see Fig. 1) according to

$$\mathbf{v}_i = \mathbf{w}_{AC} - \mathbf{w}_i, \qquad i = 1. \qquad (2B)$$

The internal wire force f_k is simply the stiffness (spring constant) of the actual wire element, k_i, times the elongation and is calculated as

$$f_{k,i} = k_i (|\mathbf{v}_i| - l_i), \qquad (3)$$

where l_i is the nominal length of the i:th wire element. Note that a positive internal force corresponds to positive elongation. If the wire is modeled not to take compression loads, the internal force is set to zero if $|\mathbf{v}_i| - l_i \leq 0$.

The wire force vector $\mathbf{f}_{w,i}$ from the i:th wire element acting on the i:th mass is then

$$\mathbf{f}_{w,i} = \left(\frac{f_{k,i}}{|\mathbf{v}_i|} \right) \mathbf{v}_i = k_i \frac{(|\mathbf{v}_i| - l_i)}{|\mathbf{v}_i|} \mathbf{v}_i. \qquad (4)$$

The total elastic force $\mathbf{f}_{e,i}$ acting on the i:th mass element is given by summation of the wire force vectors of the two adjacent wire elements according to

$$\mathbf{f}_{e,i} = \mathbf{f}_{w,i} - \mathbf{f}_{w,i+1}, \quad i = 1:n-1, \qquad (5A)$$

where the negative sign of second term is due to the definition of the $\mathbf{v}_{i+1}$ vector direction. Note that the force acting on the last mass element is simply

$$\mathbf{f}_{e,i} = \mathbf{f}_{w,i}, \qquad i = n, \qquad (5B)$$

since there is no wire element further aft. However, if the wire is connected to a towed decoy the last mass element is also subjected to the forces from the decoy.
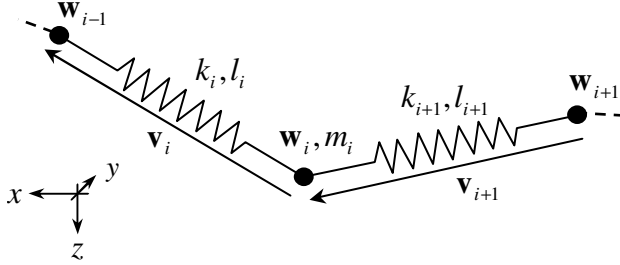
Fig. 2: Elastic wire model.

The vector of gravity forces is assumed to be independent of position and altitude and is given by the mass times the gravity vector as

$$m_i\mathbf{g}_i = \begin{Bmatrix} 0 \\ 0 \\ gm_i \end{Bmatrix}, \qquad (6)$$

where g is the acceleration of gravity.

Aerodynamics

According to Hoerner [7], the normal aerodynamic force, N, for an inclined cylinder (or wire) can be expressed as

$$N = q\, S_{\mathrm{ref}}\, C_D \sin^2(\alpha) \qquad (7)$$

where q is the dynamic pressure, S_{ref} is the reference area, C_D is the cross flow drag coefficient and α is the angle of incidence. The aerodynamic forces acting on the i:th mass element is expressed based on the velocity of the mass element and the orientation of the i:th wire element, see Fig. 3. The approximation to base the aerodynamic force on the orientation of the foregoing element may be justified since the curvature of the wire usually is relatively small compared to the wire element length. However, for very large curvatures the number

of wire elements has to be relatively large to obtain good simulation accuracy.
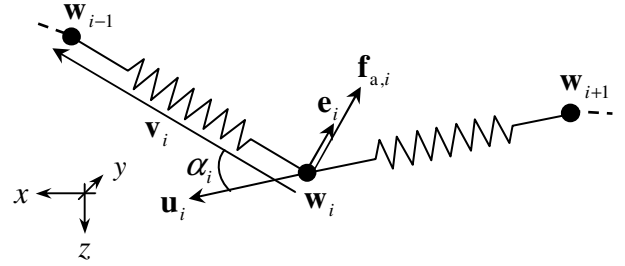
Fig. 3: Aerodynamic model.

The local angle of incidence for each wire element can be found from the expression

$$\cos(\alpha_i) = \frac{\mathbf{v}_i \cdot \mathbf{u}_i}{|\mathbf{v}_i||\mathbf{u}_i|}, \qquad (8)$$

where $\mathbf{u}_i = \dot{\mathbf{w}}_i$ is the velocity vector of the i:th mass element. A unit vector $\mathbf{e}_i$ defining the direction of the normal force can be calculated as

$$\mathbf{e}_i = \frac{(\mathbf{u}_i \times \mathbf{v}_i) \times \mathbf{v}_i}{|(\mathbf{u}_i \times \mathbf{v}_i) \times \mathbf{v}_i|}. \qquad (9)$$

Now, the vector of aerodynamic force can be expressed as

$$\mathbf{f}_{\mathrm{a},i} = \left(\frac{1}{2}\rho|\mathbf{u}_i|^2\right)(d_i\, l_i)\, C_D \sin^2(\alpha_i)\mathbf{e}_i, \qquad (10)$$

where ρ is the air density and d_i is the wire diameter. For this investigation, the Reynolds number is assumed to be subcritical and hence the cross flow drag coefficient C_D is set to 1.17 [7]. The viscous drag is for the current application considered to be small compared to the other involved forces and is therefore not included in the model.

State Space Model

It is now straightforward to assemble the wire model and to express the equations of motion

for the complete wire system on matrix form according to

$$\mathbf{M\ddot{w}} - \mathbf{f}_e(\mathbf{w}) - \mathbf{Mg} - \mathbf{f}_a(\mathbf{w}, \dot{\mathbf{w}}) = \mathbf{0}. \qquad (11)$$

The mass matrix $\mathbf{M}$ contains the mass elements on the diagonal.

For simulation purposes it is desirable to express the model on state-space form [8] according to

$$\dot{\mathbf{z}} = f(\mathbf{z}), \qquad (12)$$

where f is a function of the model state vector $\mathbf{z}$. As the system contains second order time derivatives, it is common practice to make the substitution

$$\mathbf{z} = \begin{Bmatrix} \mathbf{z}_1 \\ \mathbf{z}_2 \end{Bmatrix} = \begin{Bmatrix} \mathbf{w} \\ \dot{\mathbf{w}} \end{Bmatrix}. \qquad (13)$$

After substitution equation (11) reads

$$\mathbf{M\dot{z}}_2 - \mathbf{f}_e(\mathbf{z}_1) - \mathbf{Mg} - \mathbf{f}_a(\mathbf{z}_1, \mathbf{z}_2) = \mathbf{0}. \qquad (14)$$

The complete state-space equations for the wire can now be expressed as

$$\dot{\mathbf{z}} = \begin{Bmatrix} \dot{\mathbf{z}}_1 \\ \dot{\mathbf{z}}_2 \end{Bmatrix} = \begin{Bmatrix} \mathbf{z}_2 \\ \mathbf{M}^{-1}\left(\mathbf{f}_e(\mathbf{z}_1) + \mathbf{f}_a(\mathbf{z}_1, \mathbf{z}_2)\right) + \mathbf{g} \end{Bmatrix}. \qquad (15)$$

This equation (15) is suitable for implementation in most standard numerical simulation tools. The integration is performed from an initial state vector $\mathbf{z}_0$ until the final time.

The model outputs are primarily the positions of the wire nodes $\mathbf{w} = \mathbf{z}_1$. Additional outputs such as the internal wire force (or stress) in some point or the loads in the attachment point $\mathbf{w}_{AC}$ can easily be extracted in any time step. Also, this type of wire model can fairly easily be coupled to the dynamics of towed objects such as decoys or sensors by imposing suitable couplings and boundary conditions.

3 Implementation

The main objective with the wire model was to include it as a module in a simulator tool used for flight dynamics simulation of stores separation course of events. However, before doing this the wire model was tested and evaluated as a separate system.

Initial model evaluation

First, the developed state-space model was implemented in MATLAB [9] for testing and evaluation purposes. The simulations were performed using the standard ode45.m [9] solver. First, the structural model alone was investigated with respect to representative behavior. For this evaluation the aerodynamic forces were set to zero (using $\rho = 0$) to represent vacuum conditions. A test case with a wire, clamped at $(x, y, z) = (0, 0, 0)$, and positioned horizontally in the x-z-plane at $t = 0$ was investigated. Table 1 shows the values of the wire properties used for this simulation, referred to as Test #1.

Property	Test #1 value	Test #2 value	Unit	Description
l_{tot}	10	10	m	Total wire length
n	10	10	-	Number of wire elements
m	0.024	0.024	kg/m	Mass per length
k	1500	1500	(N/m)m	Stiffness per 1m length
d	0.002	0.002	m	Wire diameter
C_D	1.17	1.17	-	Cross flow drag coefficient
ρ	0	1.225	kg/m^3	Air density
g	9.82	9.82	m/s^2	Acceleration of gravity

Table 1: Values used for test simulations.

Fig. 4 shows the result from this simulation. The wire motion during the simulation is

illustrated by plotting of the wire position with 0.25s interval. At $t = 0$, the wire is positioned at the horizontal initial condition. The wire then accelerates due to gravity and after 1.5s the position is more or less vertical. As there is no damping, nor structural nor aerodynamic, included in the model at this point the pendulum motion of the wire will continue with time. The motion is however from this test concluded to be realistic in a qualitative sense. Note that the kinks between the individual elements of the wire are clearly visible in the figure. A finer discretization would ideally be used but the simulation is in this case mainly included as a relatively simple demonstration and reference example.
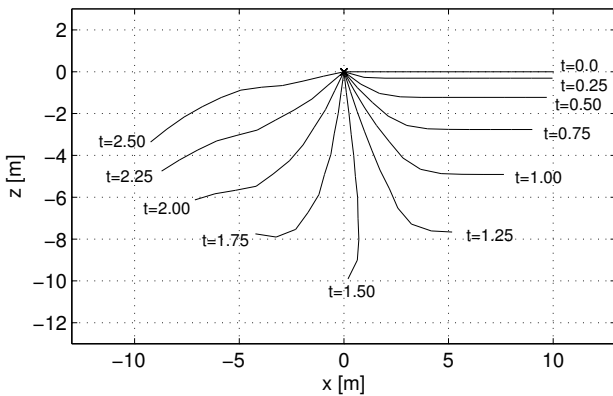
Fig. 4: Test #1 simulation of wire model in vacuum.

The next step was to perform the same simulation including the surrounding air. This test is referred to as Test #2 in Table 1. All values are kept the same as in the previous test except from the air density that was now set to 1.225kg/m^3. Fig. 5 shows the result from this simulation. It is evident that the air in this case dampens the motion somewhat compared to the vacuum condition. In this case the wire naturally approaches a vertical steady-state condition as time increases.
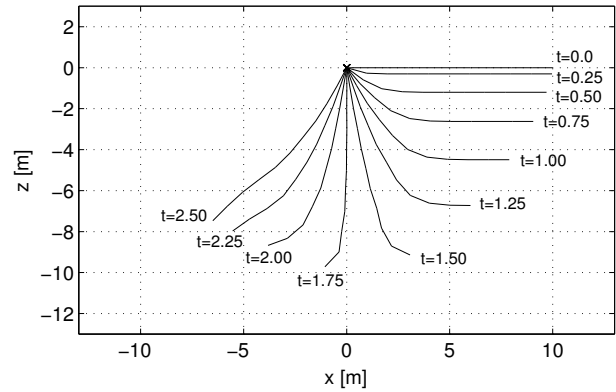
Fig. 5: Test #2 simulation with surrounding air.

Another test was made, where the steady-state condition for the wire with a point mass of 5.0kg attached to the free wire end was investigated. At this point, no additional aerodynamic drag was modeled for the point mass. The wire was attached to an aircraft flying at constant altitude with the speed of 100m/s in negative x-direction. The initial condition was the same horizontal position relative to the aircraft. Velocity was initially set to the same as for the aircraft according to $\dot{\mathbf{w}}_i = (-100, 0, 0)^{\mathrm{T}}$ for all points. After the initial transient motion, the wire stabilizes at the steady-state condition shown in Fig. 6, where the position relative to the attachment point is plotted. It is clearly shown how the gravity acting on the end point mass causes wire curvature.
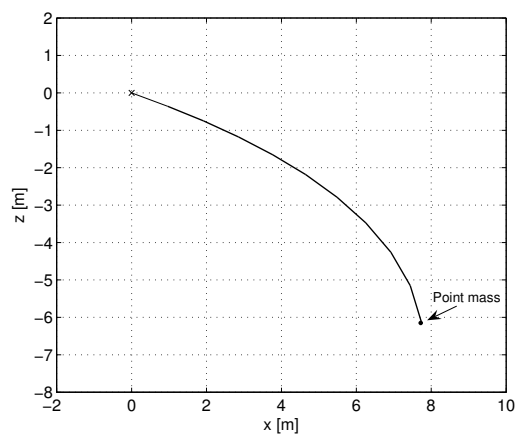
Fig. 6: Steady-state condition.

Simulator implementation

After the initial testing, the model was implemented (using C++ programming) in the simulation tool named DripDrop/Icarus developed at Saab. This implementation was first tested using the same simple examples as earlier evaluated in MATLAB. The new model was concluded to give the same result as the MATLAB version. The simulator implementation however offers significant improvement in terms of computational speed. The wire model can here be coupled to flight mechanical models of various aircraft and to 6 degree-of-freedom (6 DOF) flight mechanical models of decoys, sensors, etc. The principle and building blocks of the simulator tool are illustrated in Fig. 7. Fig. 8 shows a snapshot from the output from a simulation during a turning maneuver where the wire is attached to the fin tip of a surveillance aircraft.
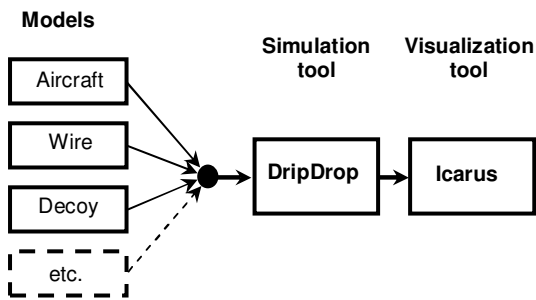
Fig. 7: Principle of stores separation simulator.
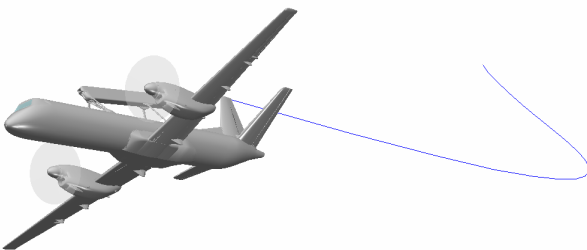
Fig. 8: Simulation with wire attached to aircraft.

4   Simulation Example

In the following, an example of an application considering the design of a towed decoy system is presented. For reasons of confidentiality no exact figures are given for properties on aircraft, wires, decoys etc. The case study should only be viewed on as an example of what the wire model can be used for in practice.

The objective with the study was to use the simulator as help for designing a towed decoy system. The system was to be installed on the Saab 2000 Airborne Early Warning (AEW) aircraft shown in Fig. 8. The aircraft is used for surveillance missions and is therefore equipped with a large radar antenna mounted at the roof of the fuselage. The aircraft is also equipped with counter measures in case of emergency. The towed decoy is winched out in case the aircraft is threatened by missiles. The decoy is towed behind the aircraft and protects the aircraft by acting as a preferential target that attracts approaching missiles.

Decoy Model

There are many different types of towed decoys with different properties in terms of size, shape and performance. The shape of the decoy investigated in this study is shown in Fig. 9. The decoy is in principle a tube filled with electronic equipment. The rear end of the decoy is shaped like a cone in order to obtain suitable aerodynamic characteristics in terms of lift, drag, and stability properties. During flight, the decoy is located in a special container mounted in the aircraft. In this example the decoy is hosted in the fin tip. For this study, a 6 DOF model of the decoy is used and coupled to the wire dynamics. Structurally the decoy is modeled as a rigid body with representative mass properties. For aerodynamics, a quasi-steady aerodynamic database is used for the simulations.
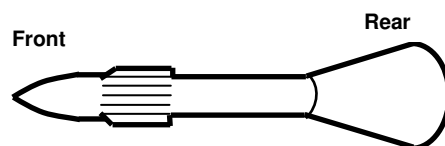
Fig. 9: Shape of the towed decoy in example.

Winch model

A special winch and brake arrangement is used to feed out the decoy when launched. The winch is dynamically modeled and this model is coupled to the dynamics of the wire. During the winch out process the length of the free wire varies with time. In this example, this is numerically solved by letting the nominal length (and consequently also the mass) of each element vary with time. Hereby, the number of states remains constant during the simulation which makes the time integration straightforward. An alternative way of handling this is to alter the number of active elements and states during launching proceeds as described in Ref. [1]. The speed of the winching process depends on the properties of the winch system and on the wire and decoy dynamics. Naturally, it is desirable to launch the decoy relatively fast if the aircraft is threatened by a missile. On the other hand it is not practical to launch the decoy to fast as this will cause large stresses in the wire when braking and high attachment loads and eventually also high risk for wire failure. The properties of the winch system are therefore tailored to get optimal performance with respect to the specific installation in mind.

Slipstream model

The Saab 2000 AEW is a twin engine turboprop aircraft as shown in Fig. 8. The engines and propellers create powerful slipstreams and exhaust flows behind the aircraft, see Fig. 10. Due to the clockwise rotation of the flow, the slipstreams from the two propellers move somewhat to the right (when viewing from behind) as they propagate downstream. This fact poses a potential risk for interaction between the towed wire and decoy and the two slipstreams. Such interaction has during some conditions been observed for earlier decoy designs on other aircraft and is naturally not desirable as this may lead to undesirable decoy trajectories and high loading on the wire and attachments.
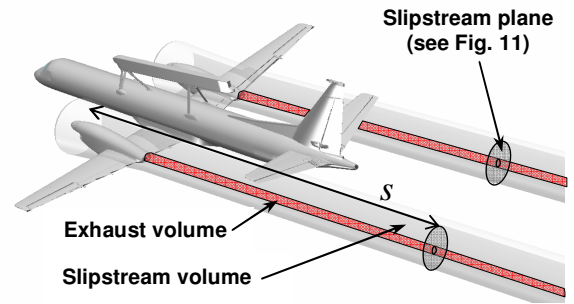
Fig. 10: Illustration of propeller slipstream.

A model of the slipstream was included in the simulation tool to enable investigations with respect to the potential interaction between the wire, decoy, and the slipstream. Basically, an additional velocity vector component is computed if some part of the wire and/or decoy is located in the slipstream or exhaust volume. The downstream propagation of the slipstream depends on the flight condition. For any point P, located in the slipstream, an additional velocity vector $\Delta\mathbf{u}$ is calculated, see Fig. 11. The additional velocity vector is built up from a rotational and an axial velocity contribution that both depend on the aircraft flight condition and on the position in the slipstream/exhaust volume according to

$$\Delta\mathbf{u} = f(\mathbf{u}_{AC}, M_{AC}, W_{AC}, T_{AC}, s, r) \qquad (16)$$

where $\mathbf{u}_{AC}$ is the aircraft velocity vector and M_{AC} is the aircraft Mach number. Moreover, the additional velocity component depends on the weight of the aircraft W_{AC} and the thrust setting T_{AC}. The position within the slipstream is given by the axial distance from the propeller disk denoted s and on the radial distance from the slipstream center r, see Fig. 11. The function parameters are for the current aircraft based on engine and propeller data and on powered wind tunnel test.
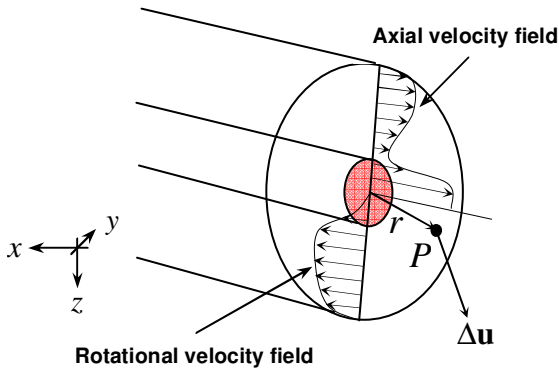
Fig. 11: Principle of slipstream model.

Results from simulations

First, an initial decoy system representing an existing design was simulated and analyzed. Several decoy launches and flight conditions were simulated. At some flight conditions, the wire and decoy were found to move into the slipstream volume. This caused violent rotational motion of the wire and decoy. A snapshot from a simulation where the wire interacts with the slipstream is shown in Fig. 12.
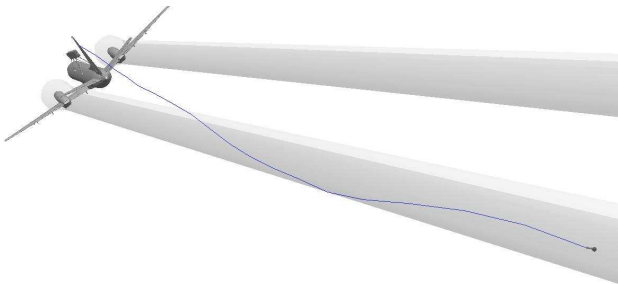
Fig. 12: Simulation with slipstream interaction.

Besides the undesirable decoy trajectory, the violent motion was also found to cause large loads and stress on the wire and large attachment loads at the fin tip. Fig. 13 shows the magnitude of the fin attachment force versus time during a certain towing maneuver. As shown, there are relatively high oscillating forces at the fin tip attachment as the wire and decoy interacts with the engine slipstream.

By careful investigation of several wire and decoy system designs and options, a new more suitable design could be found. This design was found not to interact with the slipstream during the investigated maneuvers. The magnitude of the fin tip force for this new design during the same maneuver as earlier discussed is also included in Fig. 13. As shown, the attachment force is significantly lower for this new design as the decoy and wire do not interact with the propeller slipstream.
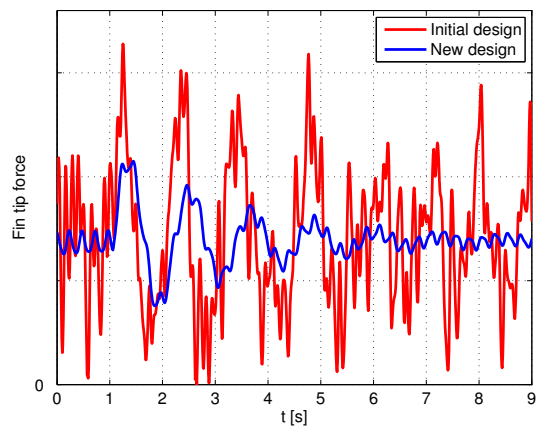
Fig. 13: Fin attachment force as function of time.

Computational remarks

The simulations described in this paper are normally performed with between 20 – 50 wire elements, giving between 120 and 300 wire states ($\mathbf{w}$ and $\dot{\mathbf{w}}$). A simulation of 30s including aircraft, decoy and winch dynamics typically takes about 60 to 120 seconds to perform on a standard PC. The most computational intensive period is during the start of the launch process. As the nominal length of the wire elements are very short (theoretically zero) at the start of the launch, the dynamic problem becomes very stiff hence requiring very small time steps for accurate integration. This is in practice handled by starting the simulations with an initial wire length of negligible practical influence on the overall course of event.

5   Conclusions

A dynamic model for simulation of towed decoy systems was developed and evaluated. The wire was modeled using a discrete approach using elastic spring elements and point masses. The aerodynamic forces acting on the wire was modeled using quasi-steady aerodynamics based on the cross flow principle. The dynamic behavior of the wire model was tested for representative behavior using some basic simulations.

The wire model was then implemented into a simulator used for stores separation analysis. As a test case, the model was used for analysis of a towed decoy system where the wire model was coupled to flight mechanical models of a surveillance aircraft and a towed decoy. Models of the decoy winch and propeller slipstream were also included in the analysis.

The simulation model was found to be a very versatile tool for evaluation of different towed decoy systems and options. Efficient simulations were performed that could reduce the time and cost for flight testing. When considering the investigated case study, the dynamics of the towed decoy was found to be significantly affected by the engine and propeller slipstream. The properties of the decoy system therefore had to be carefully chosen in order to get the desired behavior.

So far, numerical simulations have been performed and the simulation model is verified with respect to representative behavior in a qualitative sense. In order to validate the model dynamics it is however desirable to perform flight testing and to correlate experimental data with results for simulations. Such experimental validation would further increase the confidence and usefulness of the simulation model.

6   Acknowledgements

The authors would like to thank Dr. Per Weinerfelt and Yngve Sedin at Saab Aerosystems for valuable feedback and for help

with the aerodynamic data for the slipstream model.

7   References

[1] Williams, P., Sgarioto, D., and Trivailo, P. Motion planning for an aerial-towed cable system. *AIAA Paper 2005-6267*, Aug. 2005.

[2] Matuk, C. Dynamic stress in a towing wire due to forced acceleration. *Journal of Aircraft*, Vol.18, No. 6, pp. 498-499, 1981.

[3] Matuk, C. Flight tests of tow wire forces while flying a racetrack pattern. *Journal of Aircraft*, Vol.20, No. 7, pp. 623-627, 1983

[4] Clifton , J. M., Schmidt, L. V., Stuart, T. D. Dynamic modeling of a trailing wire towed by an orbiting aircraft. *Journal of Guidance, Control, and Dynamics*. Vol. 18, No. 4, pp. 875-881, 1995.

[5] Williams, P., and Trivailo, P. A study on the transitional dynamics of a towed-circular aerial cable system. *AIAA Paper 2005-6125*, Aug. 2005.

[6] Choo, Y. I., and Casarella, M. J. A survey of analytical methods for dynamic simulation of cable-body systems. *Journal of Hydrodynamics*, Vol. 7, No. 4, 1973, pp. 37-144.

[7] Hoerner, S. F., *Fluid-dynamic drag*, Hoerner Fluid Dynamics, Bakersfield, CA 93390, 1965.

[8] Khalil, H. K., *Nonlinear systems*. Third edition, Prentice-Hall. Inc., Upper Saddle River, New Jersey 07458, 2000.

[9] The MathWorks, Inc. *MATLAB High performance numeric computation and visualization software, Reference guide*. The MathWorks, Inc., Natick, Mass. 01760, 1992.

Copyright Statement